Evaluation of Long-term Deep Visual Place Recognition

Farid Alijani[1][a], Jukka Peltomäki[1][b], Jussi Puura[2], Heikki Huttunen[3][c],
Joni-Kristian Kämäräinen[1][d] and Esa Rahtu[1][e]

[1] *Tampere University, Finland*

[2] *Sandvik Mining and Construction Ltd, Finland*

[3] *Visy Oy, Finland*

Keywords: Tracking and Visual Navigation, Content-Based Indexing, Search, and Retrieval, Deep Convolutional Neural Network, Deep Learning for Visual Understanding.

Abstract: In this paper, we provide a comprehensive study on evaluating two state-of-the-art deep metric learning methods for visual place recognition. Visual place recognition is an essential component in the visual localization and the vision-based navigation where it provides an initial coarse location. It is used in variety of autonomous navigation technologies, including autonomous vehicles, drones and computer vision systems. We study recent visual place recognition and image retrieval methods and utilize them to conduct extensive and comprehensive experiments on two diverse and large long-term indoor and outdoor robot navigation datasets, e.g., COLD and Oxford Radar RobotCar along with ablation studies on the crucial parameters of the deep architectures. Our comprehensive results indicate that the methods can achieve 5 *m* of outdoor and 50 *cm* of indoor place recognition accuracy with high recall rate of 80 %.

1 INTRODUCTION

The question of “where this photo was taken?” has been a widespread research interest in multiple fields, including computer vision and robotics for many years (Zhang et al., 2020). Recently, researchers have employed advanced deep learning techniques to address this question (Masone and Caputo, 2021). The performance of a good navigation algorithm is deeply incorporated with an accurate robot localization which makes it an important research topic in robotics.

Visual place recognition is the problem of recognizing a previously visited place using the visual content and information. Similar to the image retrieval problem, the visual content can be matched with the places already stored in the gallery database. It is the first step in *hierarchical visual localization* (Sarlin et al., 2019; Xu et al., 2002) that consists of two steps: (1) coarse localization and (2) pose refinement.

Visual localization itself is a core component of *vision-based mobile robot navigation* (DeSouza and Kak, 2002; Bonin-Font et al., 2008). Our paper presents and study an extensive evaluation of two state-of-the-art deep learning methods for long-term visual place recognition in indoor and outdoor environments.

Two recent papers (Sattler et al., 2020; Pion et al., 2020) demonstrate the superior localization performance of approaches that are solely rely on deep metric learning methods, compared with the conventional engineered features or feature transforms. They measure the refined 6-Degree-of-Freedom localization accuracy in 3D, but do not factorize the contributions of (1) coarse localization and (2) pose refinement.

In this paper, we focus mainly on the coarse localization step for our contribution. In particular, we define the coarse localization as *place recognition* problem and study the performance and settings of two state-of-the-art deep metric learning architectures with two diverse and large long-term indoor and outdoor robot navigation datasets. We utilized one of the best performing CNN architectures in deep visual place recognition, *e.g.*, NetVLAD (Arandjelović et al., 2018), and another in deep image retrieval by Radenović et al. (Radenović et al., 2019).

[a] https://orcid.org/0000-0003-3928-7291
[b] https://orcid.org/0000-0002-9779-6804
[c] https://orcid.org/0000-0002-6571-0797
[d] https://orcid.org/0000-0002-5801-4371
[e] https://orcid.org/0000-0001-8767-0864

Alijani, F., Peltomäki, J., Puura, J., Huttunen, H., Kämäräinen, J. and Rahtu, E.
Evaluation of Long-term Deep Visual Place Recognition.
DOI: 10.5220/0010834700003124
In *Proceedings of the 17th International Joint Conference on Computer Vision, Imaging and Computer Graphics Theory and Applications (VISIGRAPP 2022) - Volume 5: VISAPP*, pages 437-447
ISBN: 978-989-758-555-5; ISSN: 2184-4321

Both methods utilize the deep metric learning methods to learn feature embedding and representation of images where the distance of images captured in nearby places are clearly smaller than those from the distant locations. We compare two methods using two largest available outdoor and indoor datasets: Oxford Radar RobotCar (Barnes et al., 2020) and CoSy Localization Database (COLD) (Pronobis and Caputo, 2009). We also provide an ablation study on the main performance factors of deep learning methods, the selection of the backbone network and the amount of training data.

The rest of this paper is organized as follows. Section 2 briefly discusses the related work in visual place recognition. In section 3, we provide the baseline methods utilized in our paper. Section 4 explains two real-world indoor and outdoor datasets to address the visual place recognition problem. In section 5, we show the experimental results and finally, we conclude the paper in section 6.

2 RELATED WORK

Visual Place Recognition Methods. Given a query image, an image retrieval system aims to retrieve all images from a large database containing similar features to the query image. Visual place recognition can be also interpreted as an image retrieval system which recognize a place by matching it with all places from the reference dataset. Prior research has thoroughly surveyed visual place recognition methods in recent papers. Lowry et al. (Lowry et al., 2016) define the problem and survey the classical hand-crafted or shallow learned descriptors. while Zhang et al. (Zhang et al., 2020) and Masone et al. (Masone and Caputo, 2021) focus entirely on the deep learning approaches incorporated with visual place recognition.

The conventional methods of place recognition use mainly handcrafted local features and global descriptors on their core to obtain feature descriptors. Popular local feature descriptors are SIFT (Lowe, 2004), SURF (Bay et al., 2008) and HOG (Dalal and Triggs, 2005). Commonly used global descriptors including DBoW (Galvez-López and Tardos, 2012), FAB-MAP (Cummins and Newman, 2008; Cummins and Newman, 2011) and the landmark-based relocalization approach (Williams et al., 2011), are all based on handcrafted local image features and have been widely used for visual SLAM or localization tasks.

Today, handcrafted features are being constantly outperformed by deep features that can be trained to be robust to geometric transformations and illumination changes. The deep architectures often employ pre-trained backbone networks that extract powerful semantic features. The backbone networks are trained with image classification datasets such as ImageNet (Russakovsky et al., 2015). By localization specific fine-tuning the deep features are optimized for image matching (Zhang et al., 2020; Radenovic et al., 2018).

The main objective of utilizing deep architectures for image retrieval and visual place recognition is to learn powerful and meaningful feature mapping which allows to compare images using similarity measures such as Euclidean distance or cosine similarity.

In this context, large number of architectures have been proposed: MAC (Azizpour et al., 2015), SPoC (Yandex and Lempitsky, 2015), CroW (Kalantidis et al., 2016), GeM (Radenović et al., 2019), R-MAC (Tolias et al., 2016b), modified R-MAC (Gordo et al., 2017) and NetVLAD (Arandjelović et al., 2018). For this paper, we selected two methods which perform well with public benchmarks in which the original code is publicly available: GeM (Radenović et al., 2019) and NetVLAD (Arandjelović et al., 2018).

Visual Place Recognition Datasets. For the past few years, researchers have collected and published several datasets for the problem of visual place recognition with various sensor modalities, including monocular and stereo cameras, LiDAR, IMU, radar and GNSS/INS sensors. For example, Cummins and Newman (Cummins and Newman, 2008) introduced the New College and City Centre dataset. The other popular datasets are the KITTI Odometry benchmark (Geiger et al., 2012), Canadian Adverse Driving Conditions dataset (Pitropov et al., 2021), Ford campus vision and LiDAR dataset (Pandey et al., 2011), InLoc dataset (Taira et al., 2021), extended CMU seasons dataset (Badino et al., 2011; Sattler et al., 2018), Málaga Urban dataset (Blanco-Claraco et al., 2014), Alderley dataset (Milford and Wyeth, 2012), Aachen dataset (Sattler et al., 2012) and Nordland dataset (Olid et al., 2018).

Our objective is to address both outdoor and indoor place recognition and focus more specifically on *long-term* visual place recognition, *i.e.*, how robust the deep representations are to changes over time, including illumination and weather. Therefore, we selected the two challenging datasets, COLD (Pronobis and Caputo, 2009) for indoor experiments and Oxford Radar RobotCar (Barnes et al., 2020) for outdoor experiments, that provide the same places captured in various different conditions.

3 METHODS

In this work, we concentrate on deep image representation obtained by deep convolutional neural network (CNN) architectures in which given an input an image, it produces a global descriptor, feature vector, to describe the visual content of the image. In the following, we briefly explain the processing pipelines of the Generalized Mean (GeM) by Radenović et al. (Radenović et al., 2019) that obtains good performance with image retrieval datasets and NetVLAD (Arandjelović et al., 2018) that performs well on place recognition datasets.

3.1 Radenović et al.

For training, Radenović et al. (Radenović et al., 2016; Radenović et al., 2019) adopt the Siamese neural network architecture. The Siamese architecture is trained using positive and negative image pairs and the loss function enforces large distances between negative pairs (images from two distant places) and small distances between positive pairs (images from the same place). Radenović et al. (Radenović et al., 2019) use the contrastive loss (Chopra et al., 2005) that acts on matching (positive) and non-matching (negative) pairs and is defined as follows:

$$\mathcal{L} = \begin{cases} l(\vec{f_a},\vec{f_b}) \text{ for matching images} \\ \max\left(0, M - l(\vec{f_a},\vec{f_b})\right) \text{ otherwise} \end{cases} \qquad (1)$$

where l is the pair-wise distance term (Euclidean distance) and M is the enforced minimum margin between the negative pairs. $\vec{f_a}$ and $\vec{f_b}$ denote the deep feature vectors of images I_a and I_b computed using the convolutional head of a backbone network such as AlexNet, VGGNet or ResNet.

The typical feature vector lengths K are 256, 512 or 2048, depending on the backbone. Feature vectors are global descriptors of the input images and pooled over the spatial dimensions. The feature responses are computed from K convolutional layers $\mathcal{X}_k$ following with max pooling layers that select the maximum spatial feature response from each layer of MAC vector as follows:

$$\vec{f} = [f_1 \; f_2 \; \dots \; f_K] \,,\; f_k = \max_{x\in\mathcal{X}_k}(x) \;\; . \qquad (2)$$

Radenović et al. originally used the MAC vectors (Radenović et al., 2016), but in their more recent paper (Radenović et al., 2019) compared MAC vectors to average pooling SPoC vector and Generalized Mean pooling (GeM) vector and found that GeM pooling layer provides the best average retrieval accuracy.

Radenović et al. (Radenović et al., 2019) propose GeM pooling layer to modify the MAC (Azizpour et al., 2015; Tolias et al., 2016a) and SPoC (Yandex and Lempitsky, 2015). This is a pooling layer which takes χ as an input and produces a vector $f = [f_1, f_2, f_i, ..., f_K]^T$ as an output of the pooling process which results in:

$$f_i = \left(\frac{1}{|\chi_i|}\sum_{x\in\chi_i} x^{p_i}\right)^{\frac{1}{p_i}} \qquad (3)$$

MAC and SPoC pooling methods are special cases of GeM depending on how pooling parameter p_k is derived in which $p_i \rightarrow \infty$ and $p_i = 1$ correspond to max-pooling and average pooling, respectively. The GeM feature vector is a single value per feature map and its dimension varies depending on different networks, *i.e.* $K = [256,\ 512,\ 2048]$. It also adopts a Siamese architecture to train the networks for image matching.

The Radenović et al. (Radenović et al., 2019) main pipeline is shared by the most deep metric learning approaches for image retrieval, but the unique components are the proposed *supervised whitening* post-processing and effective positive and negative *sample mining*. More details are described in (Radenović et al., 2016) and (Radenović et al., 2018) and available in the code provided by the original authors.

3.2 NetVLAD

The main advantage of Radenović et al. (Radenović et al., 2019) architecture is its straightforward implementation as it uses standard CNN layers available in PyTorch and TensorFlow libraries: conv-layers, softmax, L_2-normalization and the final aggregation layers MAC, SPoC and GeM. NetVLAD architecture, on the contrary, contains special layer that provides higher dimensional feature vector.

NetVLAD (Arandjelović et al., 2018) implements a function f as a global feature vector for a given image I_i as $f(I_i)$. This function is used to extract the feature vectors from the entire database I_i, identified as *gallery set*. Then visual search between $f(q)$, *query image*, and $f(I_i)$ takes place using Euclidean distance $d(q,I_i)$ and to obtain the top-N matches. NetVLAD is inspired by the conventional VLAD (Jégou et al., 2010) which uses handcrafted SIFT descriptors (Lowe, 2004) and uses VLAD encoding to form $f(I)$. NetVLAD is a data optimized version of VLAD for place recognition or image retrieval. NetVLAD is defined by a set of parameters θ and identified as $f_\theta(I)$ in which the Euclidean distance $d_\theta(I_i,I_j) = ||f_\theta(I_i) - f_\theta(I_j)||$ depends on the same parameters.

In order to learn the representation end-to-end, NetVLAD contains two main building blocks. (1) Cropped CNN at the last convolutional layer, identified as a dense descriptor with the output size of $H \times W \times D$, correspond to set of D-dimensional descriptors extracted at $H \times W$ spatial locations. (2) Trainable generalized VLAD layer, *e.g.*, NetVLAD which pools extracted descriptors into a fixed image representation in which its parameters trained via backpropagation.

The original VLAD image representation V is $D \times K$ matrix in which D is the dimension of the input local image descriptor $\vec{x}_i$ and K is the number of clusters. It is reshaped into a vector after L_2-normalization and (j,k) element of V is calculated as follows:

$$V(j,k) = \sum_{i=1}^{N} a_k(\vec{x}_i)(x_i(j) - c_k(j)), \qquad (4)$$

where $x_i(j)$ and $c_k(j)$ are the jth dimensions of the ith descriptor and kth cluster centers, respectively. It should be noted that $a_k(\vec{x}_i) = 0$, 1 corresponds to whether or not the descriptor $\vec{x}_i$ belongs to kth visual word. Compared to original VLAD, NetVLAD layer is differentiable thanks to its soft assignment of descriptors to multiple clusters:

$$V(j,k) = \sum_{i=1}^{N} \frac{e^{w_k^T x_i + b_k}}{\sum_{k'} e^{w_{k'}^T x_i + b_{k'}}} (x_i(j) - c_{k'}(j)) \qquad (5)$$

where w_k, b_k and c_k are gradient descent optimized parameters of the k-th cluster.

For our implementation, we obtain 64 clusters with 512-dimensional VGG16 backbone and 2048-dimensional ResNet50 backbones. Consequently, the NetVLAD feature vector dimension becomes $512 \times 64 = 32,768$ and $2048 \times 64 = 131,072$, respectively. Arandjelović et al. (Arandjelović et al., 2018) used PCA dimensionality reduction method as a post-processing stage of the implementation. However, we utilized the full size of feature vector. Since NetVLAD layer can be easily plugged into any other CNN architecture in an end-to-end manner, we investigate its performance with VGG16 and ResNet50 backbones and report the results in section 5.

Apart from designing a CNN architecture as an image representation, obtaining enough annotated training data and designing appropriate loss function for place recognition task is crucial. Following (Arandjelović et al., 2018), we adopted a weakly supervised triplet ranking loss L_θ for training. The idea of triplet ranking loss is two folds: (1) to obtain training dataset of tuples $(q, \{p_i{}^q\}, \{n_j{}^q\})$ in which for every query image q, there exists set of positives $\{p_i{}^q\}$ with at least one image matching the query and negatives $\{n_j{}^q\}$, (2) to learn an image representation f_θ so that $d_\theta(q, p_i{}^q) < d_\theta(q, n_j{}^q), \forall j$. L_θ is defined as a sum of individual losses for all n_j^q and computed as follows:

$$L_\theta = \sum_j max(\Big(|f_\theta(q) - f_\theta(p_i^q)|^2 - |f_\theta(q) - f_\theta(n_j^q)|^2 + \alpha\Big), 0), \quad (6)$$

where α is the given margin in meter. If the margin between the distance to the negative image and to the best matching positive is violated, the loss is proportional to the amount of violation.

4 DATASETS

For our experiments, we selected two publicly available and versatile outdoor and indoor datasets. We assigned three different tests, as query sequences according to their difficulty levels: (1) Test 01 with similar set of images to the gallery set, but acquired at different time; (2) Test 02 with moderately changed conditions (*e.g*, time of day or illumination) and (3) Test 03 with different set of images from the gallery set. In the following, we briefly describe the datasets and selection process of training, gallery and the three query sequences. Training data is required to fine-tune the networks for the indoor and outdoor datasets by pairing positive and negative matches from training and gallery sets.

4.1 Oxford Radar RobotCar

The Oxford Radar RobotCar dataset (Barnes et al., 2020) is a radar extension to the Oxford RobotCar dataset (Maddern et al., 2017). The dataset provides optimized ground-truth data using a Navtech CTS350-X Millimetre-Wave FMCW radar. The data acquisition was performed in January 2019 over 32 traversals in central Oxford with a total route of 280 *km* of urban driving.

This dataset addresses a wide variety of challenging conditions including weather, traffic, and lighting alterations (Figure 1). The combination of one Point Grey Bumblebee XB3 trinocular stereo and three Point Grey Grasshopper2 monocular cameras provide a 360 degree visual coverage of the scene around the vehicle platform. The Bumblebee XB3 is a 3-sensor multi-baseline IEEE-1394b stereo camera designed for improved flexibility and accuracy. It features 1.3 mega-pixel sensors with 66° horizontal FoV and 1280×960 image resolution logged at maximum frame rate of 16 *Hz*.

The three monocular Grasshopper2 cameras with fish-eye lenses mounted on the back roof of the vehicle are synchronized and obtained 1024×1024 im-

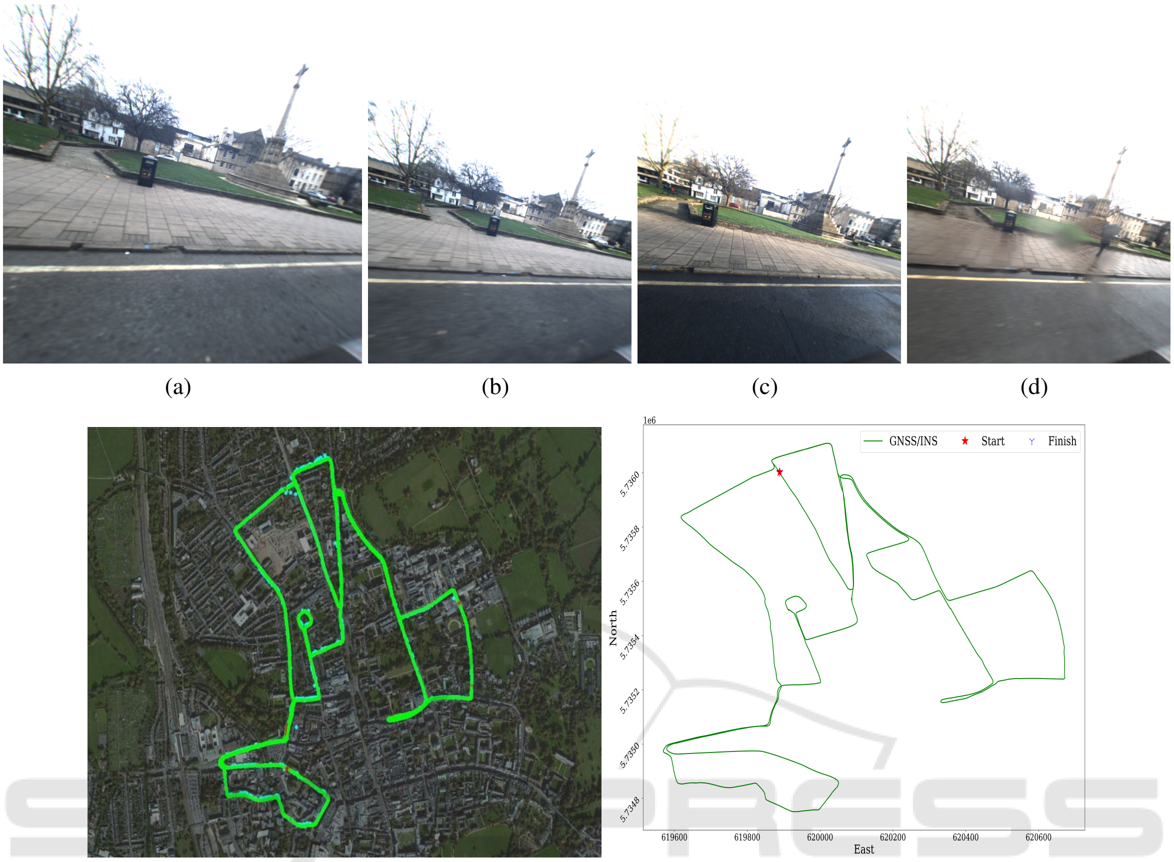

(a) (b) (c) (d)

(e) (f)

Figure 1: Examples from the Oxford Radard RobotCar outdoor dataset. Top: Images from the same location in the three selected test sequences: a) Gallery: *cloudy* b) Test 01: *cloudy* c) Test 02: *sunny* d) Test 03: *rainy* (Grasshopper2 left monocular camera). Bottom: 19 *km* route of the test sequences, e) satellite view f) GNSS/INS.

ages at average frame rate of 11.1 *Hz* with 180° horizontal FoV. To simplify our experiments, we selected images from only one of the cameras. We selected the Point Grey Grasshopper2 monocular camera, *e.g.*, left, despite the fact that using multiple cameras could potentially improve the results. The selected camera points toward the left side of the road and thus encodes the stable urban environment such as the buildings, vehicles and traffic lights.

From the dataset, we selected sequences for a training set, to perform network fine-tuning, a gallery set against which the query images from the test sequence are matched and three distinct test sets: (1) the same day but different time, (2) the different day but approximately at same time and (3) the different day and different time along with different weather conditions. Table 1 summarizes different sets used for training, gallery and testing sequences.

Table 1: The Oxford Radar RobotCar outdoor sequences used in our experiments.

Sequence	*Size*	*Date*	*Start [GMT]*	*Condition*
Train	37,724	Jan. 10 2019	11:46	Sunny
Gallery	36,660	Jan. 10 2019	12:32	Cloudy
Test 01	29,406	Jan. 10 2019	14:50	Cloudy
Test 02	32,625	Jan. 11 2019	12:26	Sunny
Test 03	28,633	Jan. 16 2019	14:15	Rainy

4.2 COLD

The CoSy Localization Database (COLD) (Pronobis and Caputo, 2009) comprises annotated data sequences, acquired using visual and laser range sensors on a mobile platform. The dataset provides a large-scale, flexible testing environment for evaluating mainly vision-based topological localization and semantic knowledge extraction methods aiming to work on mobile robots in realistic indoor scenarios.

It consists of several video sequences collected in three different indoor laboratory environments located in three different European cities: the Visual Cognitive Systems Laboratory at the University of Ljubljana, Slovenia; the Autonomous Intelligent Systems Laboratory at the University of Freiburg, Germany; and the Language Technology Laboratory at the German Research Center for Artificial Intelligence in Saarbrücken, Germany.

The COLD data acquisition was performed using three different mobile robotic platforms (an ActivMedia People Bot, an ActiveMedia Pioneer-3 and an iRobot ATRV-Mini) with two Videre Design MDCS2 digital cameras to obtain perspective and omnidirectional views. Each frame is registered with the associated absolute position recovered using laser and odometry data and annotated with a label representing the corresponding place.

The data was collected over a path when visiting several rooms and office environments and under different illumination conditions, including cloudy, night and sunny.

For our experiments, we selected the extended, *e.g.*, long path on Map B of Saarbrücken laboratory. The training sequence is Sunny-seq3, gallery sequence is Cloudy-seq1, and the three test sequences are (1) Sunny-seq1, (2) Cloudy-seq2 and (3) Night-seq3. See Figure 2 for examples. We used the captured images acquired using the monocular center camera form this setup. Table 1 summarizes different sequences used for training, gallery and testing.

Table 2: The COLD indoor sequences used in our experiments.

Sequence	*Size*	*Date*	*Start [GMT]*	*Condition*
Train	1036	July 7 2006	14:59	Sunny
Gallery	1371	July 7 2006	17:05	Cloudy
Test 01	1104	July 7 2006	14:28	Sunny
Test 02	1021	July 7 2006	18:59	Cloudy
Test 03	970	July 7 2006	20:34	Night

5 EXPERIMENTS

We organize our experiments such that they address the following research questions: (1) how accurate localization can be achieved using image retrieval methods? (2) which of the two selected deep metric learning methods performs the best (NetVlad or Radenović et al. in Section 3)? and (3) how much data specific training data is required?

Performance Metric. Similar to (Arandjelović et al., 2018), we measure the place recognition performance by the fraction of correctly matched queries. Following (Chen et al., 2011), we denote the fraction of top-N shortlisted correctly recognized candidates as recall@N. Given the available ground-truth annotations and thresholds for indoor and outdoor datasets, recall@N varies accordingly. To evaluate the performance of the methods, described in Section 3, we report only the top-1 matches, *i.e.*, recall@1 for multiple thresholds τ.

The methods in Section 3 are used to compute a feature vector representation for the given query image $f(q)$. After obtaining the image representation, a similarity score which indicates how precise two images belong to the same location is crucial to measure the performance. In this way, the feature vector is matched to all gallery image representations of $f(G_i), i = 1, 2, ..., M$ using Euclidean distance $d_{q,G_i} = ||f(q) - f(G_i)||_2$ and the smallest distance is selected as the top-1 best match. If the best match position is within the given distance threshold, *e.g.*, $d_{q,G_i} \leq \tau$, it is identified as *true positive*. In other cases, it is identified as *false positive*. We then formulate the recall as the ratio of *true positive* to the total number of the query images.

To demonstrate the generalization of our observations, we report the results of experiments using two backbones, *e.g.*, ResNet50 and VGG16. ResNet50 is a deeper architecture which contains more convolutional, pooling and fully connected layers with 50 weight layers, over 25 million parameters and 3.8 billion FLOPs (He et al., 2016). VGG16 backbone with 16 weight layers contains nearly 138 million parameters and 15.3 billion FLOPs (Simonyan and Zisserman, 2015).

Indoor Place Recognition. The results are presented in Table 3. From the results of the indoor experiments, we obtain the following findings: (1) Radenović et al. method systematically obtains better accuracy than NetVLAD method, (2) the testing performance of ResNet50 backbone is slightly better than VGG16, with a 4 % improvement on average accuracy of the recall@1 at *Test 01*, 2 % at *Test 02*, and 6.0 % at *Test 03*. However, Radenović et al. with VGG16 backbone also performs relatively well considering less computational expenses, and (3) the indoor precision drops rapidly when the threshold falls below $\tau = 50.0$ *cm*.

It simply indicates that the localization accuracy of ± 50.0 *cm* can be achieved with 80% recall@1 rate even in conditions where the query dataset is substantially different from the gallery dataset. This happens, for instance, in day *vs.* night samples.

Outdoor Place Recognition. The results are summarized in Table 4. Our findings from the outdoor experiments of Oxford Radar RobotCar dataset are similar to those of the indoor COLD database: Radenović et al. method outperforms NetVLAD method.

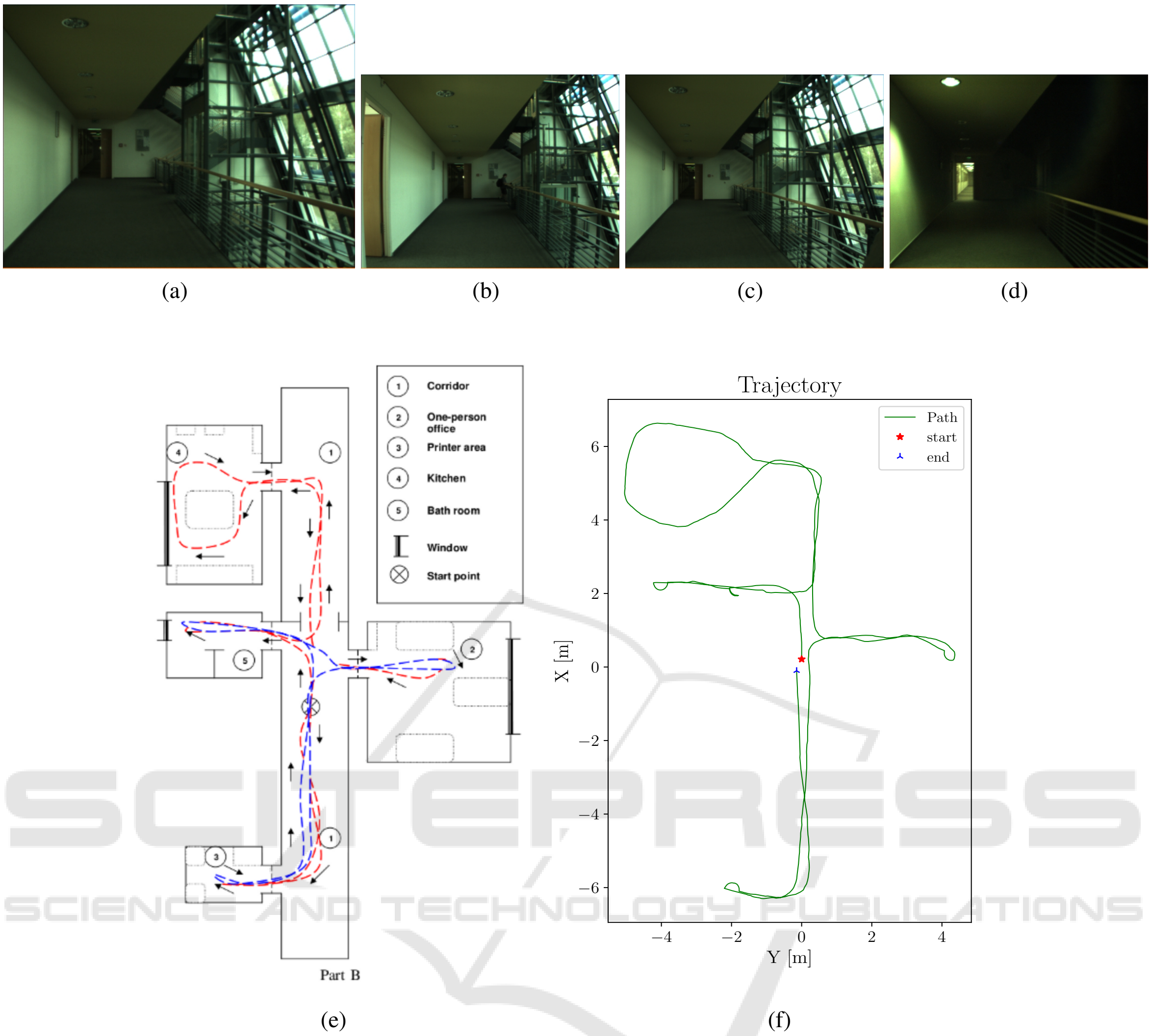

Figure 2: Examples of COLD indoor database (Pronobis and Caputo, 2009). Images of same location in different sequences: a) Gallery: *Cloudy-seq1* b) Test 01: *Sunny-seq1*, c) Test 02: *Cloudy-seq2*, d) Test 03: *Night-seq3*, e) Map view of the lab: blue dashes: standard path consisting of rooms in most typical office environments, red dashes: extended path containing rooms specific to this environment or its part, arrows: direction of driving the robot and f) Robot path of approximately 50 m.

ResNet50 provides better accuracy than the VGG16 backbone.

The higher recall@1 rates in *Test 01*, using both methods, compared to *Test 02* and *Test 03* is due to its high similarity to the gallery dataset, *e.g.*, different time during the same day. However, Radenović et al. method performs relatively better in small threshold, $\tau = 2\ m$, in *Test 03* which indicates its robustness even in extreme conditions, including night and rain.

The testing performance of ResNet50 backbone achieves a 0.2 % improvement on average accuracy of the recall@1 at *Test 01*, 4.6 % at *Test 02*, and 2.3 % at *Test 03* compared to VGG16 architecture in the corresponding tests. This surely comes with higher computation for ResNet50 backbone.

The results of the Table 4 also demonstrate that localization accuracy of ± 5.0 *m* can be achieved with the recall rate of 80% or greater for different illumination and weather conditions in an urban environment. This is reasonable due to the more versatile features of the outdoor environments, compared to the indoor environments.

The results of both Table 3 and Table 4 demonstrate that Radenović et al. method outperforms the NetVLAD in both indoor and outdoor datasets. The main clarification of better performance is the selection procedure of training image pairs for positives and negatives samples with queries forming the training tuples.

Table 3: Indoor place recognition results for the COLD Saarbrücken sequences, given various distance thresholds τ.

		COLD recall@1			
Method	BB	$\tau = 100\ cm$	$\tau = 75\ cm$	$\tau = 50\ cm$	$\tau = 25\ cm$
Test 01 (sunny)					
Radenović (Radenović et al., 2019)	VGG16	93.03	91.49	78.26	43.12
	ResNet50	**97.19**	**95.74**	**82.43**	43.39
NetVLAD (Arandjelović et al., 2018)	VGG16	92.30	89.58	76.36	41.85
	ResNet50	91.94	91.76	78.35	**44.75**
Test 02 (cloudy)					
Radenović (Radenović et al., 2019)	VGG16	94.32	**92.75**	**84.62**	**46.13**
	ResNet50	**95.20**	91.67	80.12	**46.62**
NetVLAD (Arandjelović et al., 2018)	VGG16	90.70	87.37	78.45	**46.33**
	ResNet50	93.44	89.72	79.63	45.05
Test 03 (night)					
Radenović (Radenović et al., 2019)	VGG16	82.99	82.06	75.36	44.64
	ResNet50	**91.13**	**88.97**	**80.72**	**47.32**
NetVLAD (Arandjelović et al., 2018)	VGG16	81.03	78.66	70.52	45.05
	ResNet50	82.06	79.90	71.34	44.43

In NetVLAD method, the image with the lowest descriptor distance to the query is chosen as positive pairs. In this naive approach, the network is not capable of sufficient learning from positive samples given only the GPS coordinates and camera orientation is not available. In Radenović et al. method, on the contrary, the positive samples are chosen at random from a pool of images with similar camera positions. This ensures selecting harder matching examples along with increasing variability of viewpoints. Negative samples are selected from clusters different that the cluster of the query images as clusters are non-overlapping. Non matching images with similar descriptors are selected as hard negatives.

Amount of Training Data. Finally, in this experiment we investigate to what extent the data specific fine-tuning can further improve the visual place recognition performance results. Based on the obtained results of the Table 3 and the Table 4, we assign the fixed indoor distance threshold to $\tau = 50\ cm$ and outdoor threshold to $\tau = 5\ m$. We evaluate the most challenging test sequence, *Test 03*, for both indoor and outdoor datasets.

In our experiments, we compared ResNet50 and VGG16 backbones in terms of training time using NVIDIA V100 Tensor core GPU with 32 *GB* of memory for the outdoor and indoor datasets. Our findings indicated that VGG16 is less computationally expensive and less prone to overfitting. The fine-tuning of CNN using ResNet50 backbone took approximately 9 hours and 45 minutes for the Oxford Radar RobotCar dataset with $\approx 37k$ images with size of 1024×1024 pixels and roughly 85 minutes for COLD dataset with 1036 training images of 640×480 pixels for 50 epochs and mini-batch of 5 images. However, VGG16 was slightly lighter since it took approximately 8 hours and 25 minutes for Oxford Radar RobotCar and 73 minutes for the COLD dataset.

Despite the high similarity of two backbones in the performance, we utilized VGG16 backbone. Consequently, we repeat the experiment with different amounts of training data to study how much and to what extent, the fine-tuning improves the performance. The results are presented in Table 5.

Table 5 demonstrates the absolute outperforming results of Radenović et al. method over NetVLAD with VGG16 backbone in both indoor and outdoor datasets. The accomplished performance results is regardless of how much training data is utilized for fine-tuning with new datasets. Interestingly, there is a substantial improvement from absolute zero fine-tuning data to the full training dataset (37k images) for the outdoor Oxford Radar RootCar dataset. However, there is not a significant difference for the indoor COLD dataset. This can partly be due to the fact that there are not enough training samples in the indoor dataset (approximately 1000 samples per sequence).

According to Table 5, there is also a significant improvement of the results (approximately 50 %) for the outdoor Oxford Radar RobotCar dataset when Radenović et al. method is utilized considering all the versatile characteristics of an urban environment. This is similar for the indoor COLD database even though the results of Radenović et al. method indicates approximately 10% of improvement compared to the outdoor dataset.

Table 4: Outdoor place recognition results for the Oxford Radar RobotCar dataset, given various distance thresholds τ.

		Oxford Radar RobotCar recall@1			
Method	BB	$\tau = 25\ m$	$\tau = 10\ m$	$\tau = 5\ m$	$\tau = 2\ m$
Test 01 (later time of day)					
Radenović (Radenović et al., 2019)	VGG16	**98.39**	**97.42**	**95.82**	**59.86**
	ResNet50	**98.01**	**97.23**	**95.96**	**59.94**
NetVLAD (Arandjelović et al., 2018)	VGG16	80.14	76.81	72.29	44.25
	ResNet50	92.67	89.60	84.24	52.14
Test 02 (diff. day, same time)					
Radenović (Radenović et al., 2019)	VGG16	91.37	89.37	82.16	42.02
	ResNet50	**95.11**	**93.43**	**86.91**	**48.09**
NetVLAD (Arandjelović et al., 2018)	VGG16	36.11	29.32	22.40	9.65
	ResNet50	70.54	63.35	52.42	23.83
Test 03 (diff. day and time)					
Radenović (Radenović et al., 2019)	VGG16	89.64	86.63	82.83	62.42
	ResNet50	**92.00**	**89.00**	**84.62**	**65.08**
NetVLAD (Arandjelović et al., 2018)	VGG16	33.58	28.05	23.12	13.36
	ResNet50	49.68	44.46	38.07	22.23

Furthermore, we evaluated the pre-trained models of both Radenović et al. and NetVLAD methods to investigate how much fine-tuning with our custom indoor and outdoor datasets could improve the visual place recognition performance. For both datasets, there is a significant improvement of the results. For instance, we find out that considering nearly 20 – 50 % of queries which are randomly drawn per one training epoch in the indoor COLD database could potentially enhance the performance results up to approximately 80 % during fine-tuning.

6 CONCLUSIONS

In this paper, we evaluated the performance of two state-of-the-art deep metric learning methods for the problem of visual place recognition. We used both indoor and outdoor datasets with diverse and large long-term variations, including time, illumination and weather to investigate the performance results of these methods. Our evaluation results indicate that fine-tuning the Radenović et al. (Radenović et al., 2019) method with visual place recognition datasets achieves recall rate of 80 % or greater for a given localization accuracy in the indoor and outdoor datasets, respectively.

As an alternative, we compared the obtained results of the NetVLAD (Arandjelović et al., 2018) method which is trained and fine-tuned for our custom indoor and outdoor datasets. Compared to Radenović et al. (Radenović et al., 2019) method, it revealed less robust performance due to challenging illumination and weather conditions in both indoor and outdoor datasets. Our findings from the two state-of-the-art deep learning architectures confirms that ResNet50 performs slightly better than VGG16 backbones considering the larger computational expenses. Therefore, we adopt VGG16 backbone since it is more computationally affordable.

Based on our findings from multiple experiments for both indoor and outdoor datasets, the deep architecture by Radenović et al. (Radenović et al., 2019) outperforms the NetVLAD architecture by Arandjelović et al. (Arandjelović et al., 2018) with a clear margin. The reason to clarify the better performance of Radenović et al. method lies in selection of training image pairs for the positives and the negatives samples with queries forming the training tuples. NetVLAD method suffers from the insufficient learning of the positive and the negative pairs which are selected based on the lowest and the highest descriptor distance to the query, respectively. Furthermore, our comprehensive study confirms that both deep learning architectures obtain the best results with ResNet50 backbone and by fine-tuning the architecture with data specific training data.

One possible direction for the future work can be an indoor data acquisition to a larger extent with more challenging illumination conditions, suitable for the problem of visual place recognition with more precise ground-truth and complementary sensors, *e.g.*,

Table 5: Results for different number of queries randomly drawn per one training epoch using the most challenging test sequences, *Test 03*, in both indoor and outdoor datasets. The gallery and test sets contain all images. "0" indicates that the dataset specific fine-tuning is skipped.

		Oxford Radar RobotCar ($\tau = 5\ m$)				
		recall@1				
Method	BB	37k (all)	10k	5k	2k	0
Test 03 (diff. day and time)						
Radenović (Radenović et al., 2019)	VGG16	95.82	86.10	87.53	88.91	72.62
NetVLAD (Arandjelović et al., 2018)	VGG16	80.14	13.82	20.48	21.83	23.35
		COLD ($\tau = 50\ cm$)				
		recall@1				
Method	BB	1k (all)	500	250	100	0
Test 03 (diff. day and time)						
Radenović (Radenović et al., 2019)	VGG16	77.73	78.35	80.10	77.53	77.22
NetVLAD (Arandjelović et al., 2018)	VGG16	66.80	70.52	71.86	71.13	71.55

LiDAR. It is useful to (1) investigate to what extent and how number of queries randomly drawn per one train epoch could potentially influence the recall@1 rate within certain localization accuracy and (2) whether or not sensor fusion of RGB and LiDAR could further improve the performance results in the indoor environment.

REFERENCES

Arandjelović, R., Gronat, P., Torii, A., Pajdla, T., and Sivic, J. (2018). NetVLAD: Cnn architecture for weakly supervised place recognition. *TPAMI*.

Azizpour, H., Razavian, A. S., Sullivan, J., Maki, A., and Carlsson, S. (2015). From generic to specific deep representations for visual recognition. In *2015 IEEE Conference on Computer Vision and Pattern Recognition Workshops (CVPRW)*, pages 36–45.

Badino, H., Huber, D., and Kanade, T. (2011). Visual topometric localization. In *2011 IEEE Intelligent Vehicles Symposium (IV)*, pages 794–799.

Barnes, D., Gadd, M., Murcutt, P., Newman, P., and Posner, I. (2020). The oxford radar robotcar dataset: A radar extension to the oxford robotcar dataset. In *2020 IEEE International Conference on Robotics and Automation (ICRA)*, pages 6433–6438.

Bay, H., Ess, A., Tuytelaars, T., and Van Gool, L. (2008). Speeded-up robust features (surf). *Computer Vision and Image Understanding*, 110(3):346–359. Similarity Matching in Computer Vision and Multimedia.

Blanco-Claraco, J.-L., Ángel Moreno-Dueñas, F., and González-Jiménez, J. (2014). The málaga urban dataset: High-rate stereo and lidar in a realistic urban scenario. *The International Journal of Robotics Research*, 33(2):207–214.

Bonin-Font, F., Ortiz, A., and Oliver, G. (2008). Visual navigation for mobile robots: A survey. *J Intell Robot Syst*.

Chen, D. M., Baatz, G., Köser, K., Tsai, S. S., Vedantham, R., Pylvänäinen, T., Roimela, K., Chen, X., Bach, J., Pollefeys, M., Girod, B., and Grzeszczuk, R. (2011). City-scale landmark identification on mobile devices. In *CVPR 2011*, pages 737–744.

Chopra, S., Hadsell, R., and LeCun, Y. (2005). Learning a similarity metric discriminatively with application to face verification. In *CVPR*.

Cummins, M. and Newman, P. (2008). Fab-map: Probabilistic localization and mapping in the space of appearance. *The International Journal of Robotics Research*, 27(6):647–665.

Cummins, M. and Newman, P. (2011). Appearance-only slam at large scale with fab-map 2.0. *The International Journal of Robotics Research*, 30(9):1100–1123.

Dalal, N. and Triggs, B. (2005). Histograms of oriented gradients for human detection. In *2005 IEEE Computer Society Conference on Computer Vision and Pattern Recognition (CVPR'05)*, volume 1, pages 886–893 vol. 1.

DeSouza, G. and Kak, A. (2002). Vision for mobile robot navigation: A survey. *TPAMI*.

Galvez-López, D. and Tardos, J. D. (2012). Bags of binary words for fast place recognition in image sequences. *IEEE Transactions on Robotics*, 28(5):1188–1197.

Geiger, A., Lenz, P., and Urtasun, R. (2012). Are we ready for autonomous driving? the kitti vision benchmark suite. In *2012 IEEE Conference on Computer Vision and Pattern Recognition*, pages 3354–3361.

Gordo, A., Almazán, J., Revaud, J., and Larlus, D. (2017). End-to-End Learning of Deep Visual Representations for Image Retrieval. *Int. J. Comput. Vision*, 124(2):237–254.

He, K., Zhang, X., Ren, S., and Sun, J. (2016). Deep residual learning for image recognition. In *2016 IEEE Con-*

ference on Computer Vision and Pattern Recognition (CVPR), pages 770–778.

Jégou, H., Douze, M., Schmid, C., and Pérez, P. (2010). Aggregating local descriptors into a compact image representation. In *2010 IEEE Computer Society Conference on Computer Vision and Pattern Recognition*, pages 3304–3311.

Kalantidis, Y., Mellina, C., and Osindero, S. (2016). Cross-Dimensional Weighting for Aggregated Deep Convolutional Features. In *Computer Vision – ECCV 2016 Workshops*, pages 685–701. Springer, Cham, Switzerland.

Lowe, D. G. (2004). Distinctive Image Features from Scale-Invariant Keypoints. *Int. J. Comput. Vision*, 60(2):91–110.

Lowry, S., Sünderhauf, N., Newman, P., Leonard, J. J., Cox, D., Corke, P., and Milford, M. J. (2016). Visual place recognition: A survey. *IEEE Transactions on Robotics*, 32(1):1–19.

Maddern, W., Pascoe, G., Linegar, C., and Newman, P. (2017). 1 year, 1000 km: The oxford robotcar dataset. *The International Journal of Robotics Research*, 36(1):3–15.

Masone, C. and Caputo, B. (2021). A survey on deep visual place recognition. *IEEE Access*, 9:19516–19547.

Milford, M. J. and Wyeth, G. F. (2012). Seqslam: Visual route-based navigation for sunny summer days and stormy winter nights. In *2012 IEEE International Conference on Robotics and Automation*, pages 1643–1649.

Olid, D., Fácil, J. M., and Civera, J. (2018). Single-view place recognition under seasonal changes. *CoRR*, abs/1808.06516.

Pandey, G., McBride, J. R., and Eustice, R. M. (2011). Ford campus vision and lidar data set. *The International Journal of Robotics Research*, 30(13):1543–1552.

Pion, N., Humenberger, M., Csurka, G., Cabon, Y., and Sattler, T. (2020). Benchmarking image retrieval for visual localization. In *Int. Conf. on 3D Vision (3DV)*.

Pitropov, M., Garcia, D. E., Rebello, J., Smart, M., Wang, C., Czarnecki, K., and Waslander, S. (2021). Canadian adverse driving conditions dataset. *The International Journal of Robotics Research*, 40(4-5):681–690.

Pronobis, A. and Caputo, B. (2009). Cold: The cosy localization database. *The International Journal of Robotics Research*, 28(5):588–594.

Radenović, F., Tolias, G., and Chum, O. (2019). Fine-tuning cnn image retrieval with no human annotation. *IEEE Transactions on Pattern Analysis and Machine Intelligence*, 41(7):1655–1668.

Radenovic, F., Iscen, A., Tolias, G., Avrithis, Y., and Chum, O. (2018). Revisiting oxford and paris: Large-scale image retrieval benchmarking. In *2018 IEEE/CVF Conference on Computer Vision and Pattern Recognition*, pages 5706–5715.

Radenović, F., Tolias, G., and Chum, O. (2016). CNN image retrieval learns from BoW: Unsupervised fine-tuning with hard examples. In *ECCV*.

Radenović, F., Tolias, G., and Chum, O. (2018). Deep shape matching. In *ECCV*.

Russakovsky, O., Deng, J., Su, H., Krause, J., Satheesh, S., Ma, S., Huang, Z., Karpathy, A., Khosla, A., Bernstein, M., Berg, A. C., and Fei-Fei, L. (2015). ImageNet Large Scale Visual Recognition Challenge. *International Journal of Computer Vision (IJCV)*, 115(3):211–252.

Sarlin, P., Cadena, C., Siegwart, R., and Dymczyk, M. (2019). From coarse to fine: Robust hierarchical localization at large scale. In *CVPR*.

Sattler, T., Maddern, W., Toft, C., Torii, A., Hammarstrand, L., Stenborg, E., Safari, D., Okutomi, M., Pollefeys, M., Sivic, J., Kahl, F., and Pajdla, T. (2018). Benchmarking 6dof outdoor visual localization in changing conditions. In *2018 IEEE/CVF Conference on Computer Vision and Pattern Recognition*, pages 8601–8610.

Sattler, T., Maddern, W., Toft, C., Torii, A., Hammarstrand, L., Stenborg, E., Safari, D., Okutomi, M., Pollefeys, M., Sivic, J., Kahl, F., and Pajdla, T. (2020). Benchmarking 6DOF outdoor visual localization in changing conditions. In *Int. Conf. on 3D Vision (3DV)*.

Sattler, T., Weyand, T., Leibe, B., and Kobbelt, L. (2012). Image retrieval for image-based localization revisited. In *Proceedings of the British Machine Vision Conference*, pages 76.1–76.12. BMVA Press.

Simonyan, K. and Zisserman, A. (2015). Very deep convolutional networks for large-scale image recognition. In *International Conference on Learning Representations*.

Taira, H., Okutomi, M., Sattler, T., Cimpoi, M., Pollefeys, M., Sivic, J., Pajdla, T., and Torii, A. (2021). Inloc: Indoor visual localization with dense matching and view synthesis. *IEEE Transactions on Pattern Analysis and Machine Intelligence*, 43(4):1293–1307.

Tolias, G., Sicre, R., and Jégou, H. (2016a). Particular Object Retrieval With Integral Max-Pooling of CNN Activations. In *ICL 2016 - RInternational Conference on Learning Representations*, International Conference on Learning Representations, pages 1–12, San Juan, Puerto Rico.

Tolias, G., Sicre, R., and Jégou, H. (2016b). Particular object retrieval with integral max-pooling of cnn activations.

Williams, B., Klein, G., and Reid, I. (2011). Automatic relocalization and loop closing for real-time monocular slam. *IEEE Transactions on Pattern Analysis and Machine Intelligence*, 33(9):1699–1712.

Xu, M., Snderhauf, N., and Milford, M. (2002). Vision for mobile robot navigation: A survey. *TPAMI*.

Yandex, A. B. and Lempitsky, V. (2015). Aggregating local deep features for image retrieval. In *2015 IEEE International Conference on Computer Vision (ICCV)*, pages 1269–1277.

Zhang, X., Wang, L., and Su, Y. (2020). Visual place recognition: A survey from deep learning perspective. *Pattern Recognition*, page 107760.